Modeling of wave dispersion along cylindrical structures using the spectral method

Florian Karpfinger[a] and Boris Gurevich[b]
Department of Exploration Geophysics, Curtin University, GPO Box U1987, Perth, Western Australia 6845, Australia

Andrey Bakulin[c]
WesternGeco, 10001 Richmond Ave., Houston, Texas 77042

(Received 20 November 2007; accepted 9 May 2008)

Algorithm and code are presented that solve dispersion equations for cylindrically layered media consisting of an arbitrary number of elastic and fluid layers. The algorithm is based on the spectral method which discretizes the underlying wave equations with the help of spectral differentiation matrices and solves the corresponding equations as a generalized eigenvalue problem. For a given frequency the eigenvalues correspond to the wave numbers of different modes. The advantage of this technique is that it is easy to implement, especially for cases where traditional root-finding methods are strongly limited or hard to realize, i.e., for attenuative, anisotropic, and poroelastic media. The application of the new approach is illustrated using models of an elastic cylinder and a fluid-filled tube. The dispersion curves so produced are in good agreement with analytical results, which confirms the accuracy of the method. Particle displacement profiles of the fundamental mode in a free solid cylinder are computed for a range of frequencies.
 [DOI: 10.1121/1.2940577]

PACS number(s): 43.40.At, 43.58.Ta, 43.35.Cg, 43.20.Hq [LLT] Pages: 859–865

I. INTRODUCTION

Modeling different wave modes propagating along a cylindrical borehole is important for the understanding and quantitative interpretation of borehole sonic and seismic measurements. Numerous different modes such as head waves, trapped modes, and surface waves can be observed in these structures. All these modes are frequency dependent. In sonic-logging recordings these modes overlap and are often hard to identify. In order to separate different borehole modes it is useful to analyze their dispersive characteristics.

Traditionally, mode dispersion was studied by finding roots of analytical dispersion equations. The method has a long history. By the end of the 19th century Pochhammer[1] and Chree[2] investigated the wave propagation in free elastic rods. These solutions are presented in detail by Love (Ref. 3, Sec. 201) and Kolsky (Ref. 4, Chap. 3). Numerical solutions to the Pochhammer–Chree equation are presented, for example, by Bancroft.[5]

Another case which was investigated by different authors is that of a hollow[6–8] and fluid-filled[9–11] cylindrical shell.

The root-finding method, however, becomes difficult to implement when the number of cylindrical layers and/or modes of interest becomes large.[12] The separation of different roots in the complex plane becomes even more challenging when inelastic effects need to be taken into account, such as in the case of a cylinder filled with a viscoelastic fluid[13–15] or poroelastic structures.[16–18]

An alternative approach to model two-dimensional circular structures was recently introduced by Adamou and Craster[19] based on spectral methods. The idea of this method is to solve the underlying differential equations by numerical interpolation using orthogonal polynomials and spectral differentiation matrices (DMs). The advantage of this approach is that it is much faster and easier to implement than conventional root-finding methods, especially for attenuating, poroelastic, or anisotropic structures.

In this paper we extend the concept of the spectral method for wave propagation along circular cylindrical structures, and compare the results with known analytical solutions. In Sec. II, the underlying equations in cylindrical coordinates and the eigenvalue problem are formulated for a free solid cylinder. In Sec. III, the solution of the eigenvalue problem for an elastic cylinder is described using the spectral method. Numerical results are presented in the form of dispersion curves. In Sec. IV the approach is extended to multiple layers. The dispersion curves are displayed for the case of a fluid filled tube. In Sec. V, displacement profiles are computed for various frequencies of the fundamental mode propagating in the free solid cylinder.

II. THEORY

A. Equations of motion

We first introduce the spectral method for the simplest case of axisymmetric wave propagation along a free solid bar. The dynamics of the cylinder is analyzed in cylindrical

[a]Electronic mail: florian.karpfinger@postgrad.curtin.edu.au
[b]Electronic mail: boris.gurevich@geophy.curtin.edu.au. Also at CSIRO Petroleum, Bentley, Western Australia
[c]Electronic mail: abakulin@slb.com

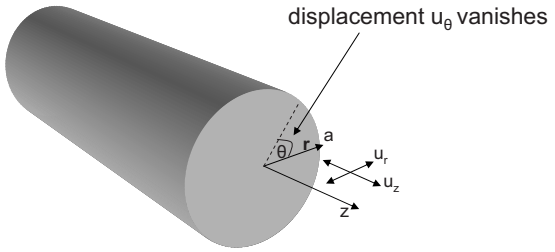

FIG. 1. Geometry of a free solid bar, displaying the coordinate system which reduces to (r,z) and the displacement field (u_r,u_z) for axisymmetric wave propagation.

coordinates (r,θ,z) (Fig. 1). For axisymmetric motion the transverse component u_θ of the displacement field $\mathbf{u}=(u_r,u_\theta,u_z)$ is identically zero, while its radial and axial components u_r and u_z are independent of θ.

For the analysis of the wave propagation it is convenient to introduce displacement potentials

$$u_r = \partial_r\phi - \partial_z\psi_\theta, \tag{1}$$

$$u_z = \partial_z\phi + r^{-1}\partial_r(r\psi_\theta), \tag{2}$$

where ϕ is the scalar potential and ψ_θ is the transverse component of the vector potential $\boldsymbol{\psi}$, ∂_x is a shortcut for the partial derivative $\partial/\partial x$. For axisymmetric motion ψ_θ is the only nonzero component of $\boldsymbol{\psi}$:

$$\psi = (0,\psi_\theta,0)^T, \tag{3}$$

where ψ_θ can in turn be written as

$$\psi_\theta = -\partial_r\eta, \tag{4}$$

so that

$$\boldsymbol{\psi} = \nabla\times(\eta\mathbf{e}_z), \tag{5}$$

where $\mathbf{e}_z$ is the unit vector in z direction.

The equations of axisymmetric motion can be written in the form (see Ref. 20, Sec. 2.13)

$$\nabla^2\phi = \frac{1}{v_p^2}\partial_t^2\phi, \tag{6}$$

$$\left(\nabla^2 - \frac{1}{r^2}\right)\psi_\theta = \frac{1}{v_p^2}\partial_t^2\psi_\theta, \tag{7}$$

where v_p is the P-wave velocity, v_s is S-wave velocity, t is time, and ∇^2 is Laplace operator,

$$\nabla^2 = \partial_r^2 + r^{-1}\partial_r + \partial_z^2. \tag{8}$$

The motion of the cylinder can be found from the solution of Eqs. (6) and (7) subject to the boundary conditions on the displacements and stress tractions on the free surface of the cylinder. The displacements are given by Eqs. (1) and (2). The normal and tangential stress tractions are related to displacements using the Hooke's law,

$$\sigma_{rr} = \lambda\Delta + 2\mu\partial_r u_r, \tag{9}$$

and

$$\sigma_{rz} = \mu(\partial_z u_r + \partial_r u_z), \tag{10}$$

where $\Delta = \partial_r u_r + \partial_r r^{-1} + \partial_z u_z$ denotes the dilatation in cylindrical $r-z$ coordinates, λ and μ are the Lame parameters.

We consider the propagation of an infinite train of sinusoidal waves along the z axis of the cylinder, which is a harmonic function of z and t of the form

$$\phi = \Phi e^{i(k_z z-\omega t)}, \quad \psi_\theta = \Psi e^{i(k_z z-\omega t)}, \tag{11}$$

where ω is the angular frequency, k_z the axial wave number, and U and W are the amplitudes which are functions of r and θ. From Eq. (11) it follows that $\partial_t\phi = -\omega\phi$ and $\partial_z\phi = ik_z\phi$, etc.

B. Helmholtz equations

The two wave equations [Eqs. (6) and (7)] transformed into the $\omega-k_z$ domain by introducing Eq. (11) and dropping $e^{i(k_z z-\omega t)}$ become

$$\underbrace{\left(\partial_r^2 + r^{-1}\partial_r + \frac{\omega^2}{v_p^2}\right)}_{\mathfrak{L}_{v_p}}\Phi = k_z^2\Phi, \tag{12}$$

$$\underbrace{\left(\frac{\partial^2}{\partial r^2} + \frac{1}{r}\frac{\partial}{\partial r} - \frac{1}{r^2} + \frac{\omega^2}{v_s^2}\right)}_{\mathfrak{L}_{v_s}}\Psi = k_z^2\Psi. \tag{13}$$

Equations (12) and (13) are now ordinary differential equations containing derivatives with respect to r only and coefficients depending on frequency ω and axial wave number k_z. The aim is to find a relation between ω and k_z. This means finding a k_z for a given ω or vice versa. This can be done by solving Eqs. (12) and (13) as an eigenvalue problem so that the wave number k_z^2 represents the eigenvalue and the potentials $\Phi(r)$ and $\Psi(r)$ are the eigenvectors. Alternatively, we could rearrange Eqs. (12) and (13) so that the terms with k_z appear on the left-hand side and with ω on the right-hand side, which will give an eigenvalue problem for ω^2. For linear elasticity both approaches must give identical results.[19] However for more complicated media (say, viscoelastic or poroelastic) it is advantageous to look for k_z as a function of ω as coefficients of governing equations may themselves explicitly depend on ω.

C. Boundary conditions

The solution of Eqs. (12) and (13) should be solved subject to boundary conditions on the surface of the cylinder. In order to apply the boundary conditions, the displacements and stress components have to be expressed independent of the axial wave number k_z.

The radial and axial displacement components u_r and u_z can be expressed by substituting Eq. (11) into Eqs. (1) and (2),

$$u_r = \partial_r\Phi - \hat{\Psi}, \tag{14}$$

$$\hat{u}_z = \underbrace{-k_z^2\Phi}_{\mathfrak{L}_{v_p}\Phi} + (\partial_r + r^{-1})\hat{\Psi}, \tag{15}$$

where $\hat{\Psi} = ik_z\Psi$ and $\hat{u}_z = ik_z u_z$.

These expressions are used to make the stress components σ_{rr} and σ_{rz} [Eqs. (9) and (10)] solely dependent on the potentials Φ and $\hat{\Psi}$. This yields after some manipulations

$$\sigma_{rr} = \left[-\lambda\left(r^{-2} + \frac{\omega^2}{v_p^2}\right) + 2\mu\partial_r^2\right]\Phi + 2\mu\partial_r\hat{\Psi}, \tag{16}$$

$$\hat{\sigma}_{rz} = -2\mu\left(\partial_r^3 + r^{-1}\partial_r^2 - r^{-2}\partial_r + \frac{\omega^2}{v_p^2}\partial_r\right)\Phi + \mu\left(2\partial_r^2 + 2r^{-1}\partial_r - 2r^{-2} + \frac{\omega^2}{v_s^2}\right)\hat{\Psi}, \tag{17}$$

where $\hat{\sigma}_{rz} = ik_z\sigma_{rz}$. Equations (12)–(17) fully describe the problem of any vibrating cylindrical structures in the r–z plane.

The classical way to solve such problems would be the so-called *root-finding* approach. A general solution to Eqs. (12) and (13) is found, which is a combination of Bessel functions of different order. Substituting the solution into the boundary conditions yields a homogeneous system of linear algebraic equations. In order for this system to have nontrivial solutions, the determinant of its matrix M must be equal to zero, $\det M(\omega, k_z) = 0$. This is called the frequency equation. The roots of this equation yield the dispersion relation $\omega(k_z)$. Since wave solutions in cylindrical coordinates contain various Bessel functions, it is often quite difficult to isolate and determine the various roots. Solving the frequency equation gets even more complicated in the case of leaky modes or lossy structures where solutions of the dispersion relation should be found in the complex plane.

In Sec. III an alternative approach, based on the spectral method, is presented.

III. SPECTRAL METHOD FOR AN ELASTIC CYLINDER

The spectral method bypasses the difficulties and solves the underlying Helmholtz equations numerically. For elastic wave propagation this was first implemented by Adamou and Craster,[19] who investigated circumferential waves in an elastic annulus (motion independent of r and z, see Fig. 1). In this study we extend the spectral method to axisymmetric longitudinal modes.

Subsequently the method is straightforwardly extended to the case of arbitrary n-layered fluid–solid media. The eigenvectors correspond to the potentials Φ and Ψ which are used to compute the mode shapes.

A. Polynomial interpolation

In order to solve the eigenvalue problem (12) and (13) numerically represent functions $\Phi(r)$ and $\Psi(r)$ by Chebychev polynomials. The advantage of this approach is that the derivatives of these polynomials can be computed exactly using so-called differentiation matrices. Consider a function $f(r)$ evaluated at N interpolation points, which is represented by a vector $\mathbf{f}$ of length N. This interpolated function $\mathbf{f}^{(m)}$ is connected to its mth derivative $\mathbf{f}$ through

$$\begin{pmatrix} f_1^{(m)} \\ f_2^{(m)} \\ \vdots \\ f_N^{(m)} \end{pmatrix} \approx \underbrace{\begin{pmatrix} D_{11}^{(m)} & D_{12}^{(m)} & \cdots & D_{1N}^{(m)} \\ D_{21}^{(m)} & \ddots & & \vdots \\ \vdots & & \ddots & \vdots \\ D_{N1}^{(m)} & \cdots & \cdots & D_{NN}^{(m)} \end{pmatrix}}_{D^{(m)}} \cdot \begin{pmatrix} f_1 \\ f_2 \\ \vdots \\ f_N \end{pmatrix}. \tag{18}$$

This is, the mth derivative of $\mathbf{f}$ can be calculated by multiplying $\mathbf{f}$ with the $N \times N$ matrix $D^{(m)}$, which represents the DM. The N interpolation points, which are, in our case, evaluated along the radius r of the cylinder, are the N maxima of the Chebyshev polynomial of the Nth order. The Chebyshev DMs are calculated using the recursive formula for the derivatives of Chebyshev polynomials. The advantage of this approach is that the derivatives of the polynomials can be computed exactly.

The DMs may be generated using the MATLAB routine CHEBDIF.[21] The discretized $\mathbf{r}$ vector and the calculated DMs are now used to represent the differential operator $\mathfrak{L}_{vp}$ as an $N \times N$ matrix,

$$L_{v_p} = D^{(2)} + \mathrm{diag}\left(\frac{1}{r}\right)D^{(1)} + \left(\frac{\omega^2}{v_p^2}\right)\mathbf{I}, \tag{19}$$

where $\mathrm{diag}(g(r))$ represents a matrix with the elements of a vector $\mathbf{g}(\mathbf{r})$ on the leading diagonal and zeros elsewhere. $\mathbf{I}$ is the identity tensor of size $N \times N$. In the same way matrix representations for all equations of motion as well as displacement and stress components are constructed.

B. Eigenvalue problem

The Helmholtz equations (12) and (13) can be combined as a matrix equation of the following form:

$$\underbrace{\begin{pmatrix} \mathfrak{L}_{v_p} & 0 \\ 0 & \mathfrak{L}_{v_s} \end{pmatrix}}_{\mathfrak{L}} \underbrace{\begin{pmatrix} \Phi \\ \hat{\Psi} \end{pmatrix}}_{\boldsymbol{\Theta}} = k_z^2 \begin{pmatrix} \Phi \\ \hat{\Psi} \end{pmatrix}. \tag{20}$$

To solve Eq. (20) as an eigenvalue problem numerically, the differential operator matrix $\mathfrak{L}$ has to be discretized in analogy to Eq. (19). Equation (20) can now be expressed in terms of DMs where L now is a matrix of size $2N \times 2N$ matrix,

$$\underbrace{\begin{pmatrix} L_{v_p} & 0 \\ 0 & L_{v_s} \end{pmatrix}}_{L} \boldsymbol{\Theta} = k_z^2 \boldsymbol{\Theta}, \tag{21}$$

where

$$L_{vp} = D^{(2)} + \mathrm{diag}\left(\frac{1}{r}\right)D^{(1)} + \left(\frac{\omega^2}{v_p^2}\right)\mathrm{I}, \tag{22}$$

$$L_{vs} = D^{(2)} + \mathrm{diag}\left(\frac{1}{r}\right)D^{(1)} - \left(\frac{1}{r^2}\right)\mathrm{I} + \left(\frac{\omega^2}{v_p^2}\right)\mathrm{I}. \tag{23}$$

Furthermore, the boundary conditions, also expressed in form of DMs have to be substituted. For a free solid bar, the

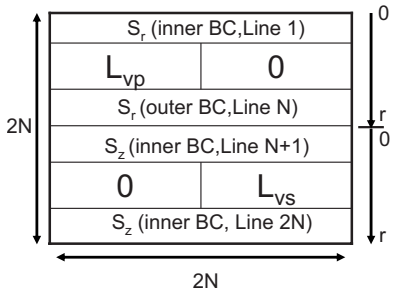

FIG. 2. Structure of the $\tilde{L}$ matrix for a cylinder.

stress-free boundary conditions are assumed at $r=a$, which means $\sigma_{rr}|_{r=a}=\sigma_{rr}|_{r=a}=0$. σ_{rr} is the normal stress in radial direction and σ_{rz} is the radial shear stress acting in z direction.

The expressions for the stress components σ_{rr} [Eq. (16)] and σ_{rz} [Eq. (17)] can also be expressed using the DMs: The resulting equations can be written in a matrix form

$$\begin{pmatrix} \sigma_{rr} \\ \hat{\sigma}_{rz} \end{pmatrix} = \underbrace{\begin{pmatrix} S_{r\Phi} & S_{r\Psi} \\ S_{z\Phi} & S_{z\Psi} \end{pmatrix}}_{S} \begin{pmatrix} \Phi \\ \hat{\Psi} \end{pmatrix}, \tag{24}$$

where submatrices $S_{r\Phi}S_{r\Psi}S_{z\Phi}S_{z\Psi}$ are

$$S_{r\Phi} = -\lambda[\mathrm{diag}(r^{-2}) + \omega^2/v_p^2] + 2\mu D^{(2)}, \tag{25}$$

$$S_{z\Phi} = 2\mu D^{(1)}, \tag{26}$$

$$S_{r\hat{\Psi}} = -2\mu\left[D^{(3)} + \mathrm{diag}\left(\frac{1}{r}\right)D^{(2)} \right. \tag{27}$$

$$\left. - \mathrm{diag}\left(\frac{1}{r^2}\right)D^{(1)} + (\omega^2/v_p^2)I \right], \tag{28}$$

$$S_{z\hat{\Psi}} = \mu\left[2D^{(2)} + 2\,\mathrm{diag}\left(\frac{1}{r}\right)D^{(1)} \right. \tag{29}$$

$$\left. - \mathrm{diag}\left(\frac{1}{r^2}\right) + (\omega^2/v_s^2)I \right]. \tag{30}$$

The last step is to embed appropriate boundary conditions in the matrix representation and replace matrix L with matrix $\tilde{L}$ as shown in Fig. 2. The lines in the L matrix in Eq. (21) corresponding to $r=a$ will be replaced by the corresponding lines of the S matrix. In order to fulfill the stress free boundary conditions, the corresponding values on the right-hand side have to be set equal to zero. In addition, for the lines at $r=0$ the same has to be done. The reason for that is that due to the singularities of the equations at $r=0$ we have to consider a hollow cylinder with a very small inner radius, which is a limiting case for a solid cylinder.

This can be done by introducing a matrix Q on the right-hand side of Eq. (21),

$$\tilde{L}\boldsymbol{\Theta} = k_z^2 Q\boldsymbol{\Theta}, \tag{31}$$

which is a $2N\times 2N$ matrix and defined as follows:

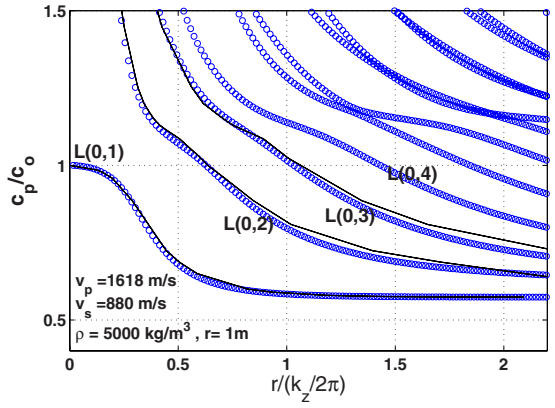

FIG. 3. (Color online) Dispersion curves of an elastic cylinder (circles). x axis: Wave-number-radius product, y axis: Phase velocity $v_{\mathrm{ph}}=\omega/k_z$ normalized by the bar velocity $v_0^2=E/\rho$ where E is the Young's modulus and ρ is density [compare with Davies (Ref. 22, Sec. 11, Fig. 13, lines)].

$$Q = \begin{pmatrix} M & 0 \\ 0 & M \end{pmatrix}. \tag{32}$$

Here M is a diagonal matrix which has the following form:

$$M = \begin{pmatrix} 0 & & & \\ & 1 & & \\ & & \ddots & \\ & & & 1 \\ & & & & 0 \end{pmatrix}. \tag{33}$$

Equation (31) is a generalized eigenvalue problem, which means that we cannot find the inverse M^{-1} as $\det(M)=0$. But generalized eigenvalue problems can be solved using the MATLAB routine EIG$(\tilde{L},Q)$ for instance.

In the next section this approach can be extended to n arbitrary cylindrical fluid and solid layers.

C. Dispersion curves

Let us illustrate the results produced by this approach in the form of dispersion curves (Fig. 3). To compare with previous results obtained by root-finding techniques, we use a model presented by Davies.[22] In Fig. 3 the dispersion curves for a free solid bar are computed (circles) with the parameters shown in the picture. These curves are in good agreement (lines) with the dispersion curves provided in Davies,[22] (Fig. 4) which were calculated analytically using root-finding techniques. The fundamental mode $L(0,1)$ behaves like a pure extensional mode for low frequencies and propagates with the velocity $\sqrt{E/\rho}$ where E is the Young's modulus and ρ is density. For higher frequencies the mode propagates like a Rayleigh wave on the cylinder surface. The higher modes $(L(0,1)\ldots L(0,n))$ have cut-off frequencies, which means they do not exist below these frequencies. For very high frequencies they tend to propagate close to the Rayleigh velocity.

IV. MULTIPLE LAYERS

The above-described approach can be extended to n cylindrical fluid and solid layers (see Fig. 4). Each of the n

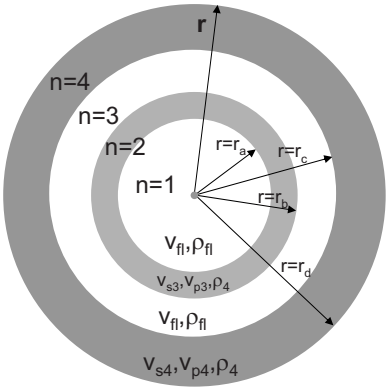

FIG. 4. Geometry of a model with four cylindrical layers. The layer index is $n=1-4$ numbered from the center to the surface of the bar. The layers are either nonviscous fluid $(v_{\mathrm{fl}},\rho_{\mathrm{fl}})$ or elastic solid $(v_{pn},v_{sn},\rho_{\mathrm{fl}})$.

layers has P- and S-wave velocities $(v_{p_1},\ldots,v_{p_n},v_{s_1},\ldots,v_{s_n})$ and densities $\rho_1,\ldots,\rho_n$. In this work we represent the fluid layers as solids with very small shear velocity. For each of the layers the matrix L_n is constructed in analogy to Eq. (21). These matrices are combined in a diagonal matrix of the size $n2N\times n2N$ which has the form

$$L=\begin{pmatrix} L_1 & 0 & 0 \\ 0 & \ddots & 0 \\ 0 & 0 & L_n \end{pmatrix}. \tag{34}$$

The same procedure has to be followed for the stress components S_n [see Eq. (24)] and for each layer n which are finally combined in a matrix S of same size as L. A similar matrix U is computed for the displacement components.

For the case of layering, additional conditions of continuity of displacements and stresses have to be introduced,

$$[\sigma_{rr}]|_{r=r_i}=[\sigma_{rz}]|_{r=r_i}=0, \tag{35}$$

$$[u_r]|_{r=r_i}=[u_z]|_{r=r_i}=0, \tag{36}$$

where r_i indicates the position of the interface of the nth layer with $i=a,b,\ldots$.

The interface conditions are introduced as the vanishing differences of the displacements and stresses of the corresponding layers. It is convenient to apply the conditions as illustrated in Fig. 5, which shows in which lines of the L matrix for n layers all boundary conditions have to be introduced. The stress-free boundary conditions on the inner and outer boundary are introduced in the L matrix the same way as for a free cylinder in the rows $(1, N+1, n2N-N$ and $n2N)$.

This means that the elements of S and U representing the interpolation points of the inner and outer boundary and the interfaces replace the corresponding rows in the L matrix, which is now referred to as $\tilde{L}$. The eigenvalue problem can now be formulated analogous to Eq. (31) and solved using a generalized eigenvalue routine.

Dispersion curves: Fluid-filled cylinder. The second example (Fig. 6) is a two-layer model: A fluid-filled cylinder. The dispersion curves were originally calculated by Del Grosso and McGill.[9] Here the dispersion curves (lines) were computed by Sidorov using the *root-finding* technique analogous to that of Ref. 9. Again we were able to reproduce these results accurately using the spectral method. The dispersion curves referred to as ETn are for stress free surface boundary conditions, while the Rn modes were computed for rigid surface boundary conditions.

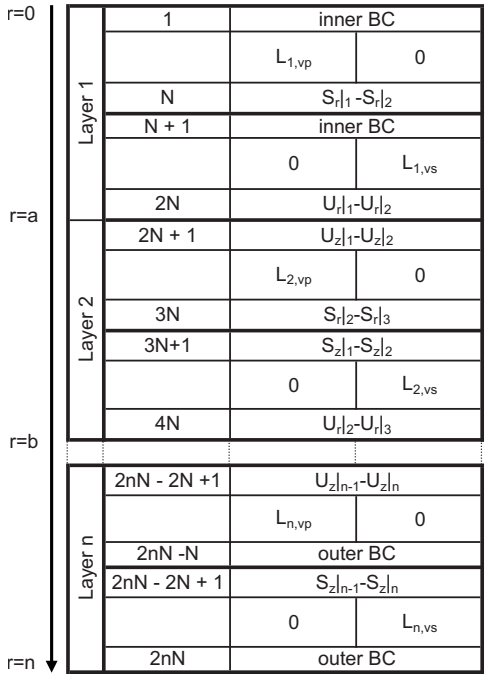

FIG. 5. Structure of the matrix $\tilde{L}$ for n layers.

In the case of a stress free surface there exist two fundamental modes starting from zero frequency: The first one (ET0) is commonly referred to as a tube wave or Stoneley wave, while the second (ET1) is an analog of a (longitudinal) plate or extensional wave. Mode ET1 only weakly depends on the fluid properties and disappears when the thickness of the cylinder wall increases to infinity or the outer boundary of the cylinder becomes rigid (Rn).

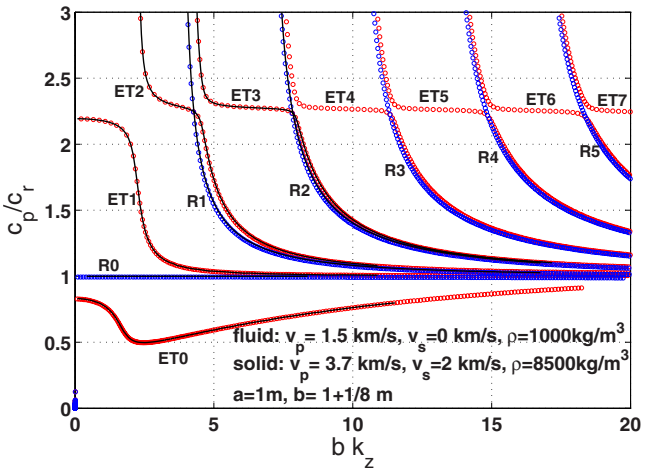

FIG. 6. (Color online) Dispersion curves for a hollow cylinder filled with nonviscous fluid. Thickness of the cylinder wall: 0.125 m. Modes in elastic tube with stress-free outer boundary: ET_n, whereas modes for pipe with rigid outer boundary: R_n. Phase velocity v_{ph} is normalized by the velocity of the fluid $(v_{p,\mathrm{fl}})$ [compare with Del Grosso and McGill (Ref. 9), lines].

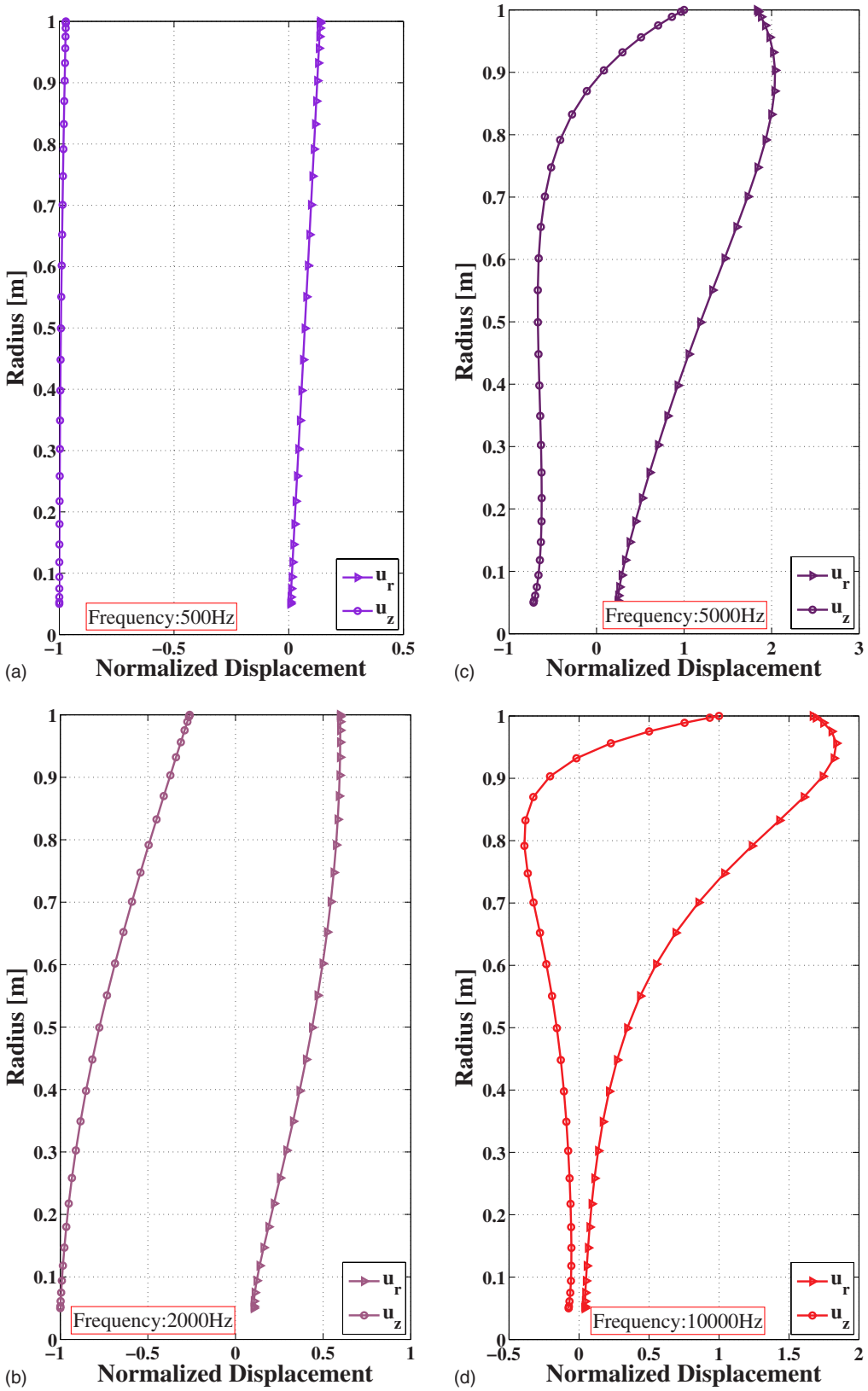

FIG. 7. (Color online) Particle displacement profiles of the fundamental longitudinal mode $L(0,1)$ for (a) 500 Hz, (b) 2000 Hz, (c) 5000 Hz, (d) 10 000 Hz. x axis: Normalized $u_r=|u_r|$ (triangle) and $u_z=i|u_z|$ (circle) displacement. y axis: Bar radius from 0 m (center of bar) to 1 m (surface of bar).

V. PARTICLE DISPLACEMENT PROFILES

In addition to eigenvalues representing dispersion curves, we also obtain eigenvectors representing the potentials Φ and Ψ. They allow the computation of the mode shapes, that is the distribution of field quantities for each mode like displacements, stresses, power flow, etc., along the radius of the cylinder. Figure 7 shows the displacements (u_r, u_z) which can be easily computed using the eigenvectors and Eqs. (4) and (5). In order to display the particle displacement profiles u_r and u_z are calculated along the radius for a

certain frequency. These values are normalized by the maximum absolute value of the u_z displacement. Finally the radial displacement is plotted as $u_r = |u_r|$ and the longitudinal displacement as $u_z = \mathrm{Im}|u_z|$.

For the illustration of the displacement profiles we have chosen the fundamental mode $L(0,1)$ propagating in a free solid cylinder (see Fig. 1). The particle motions u_r and u_z are computed for four different frequencies. Figures 7(a)–7(d) display the displacement profiles for u_r and u_z for the different frequencies.

For low frequencies (500 Hz) [Fig. 7(a)] the wave propagates like a longitudinal body wave. Consequently the particle motion is in the axial direction mainly and uniform throughout the radius of the cylinder. The radial displacement is very small.

In Fig. 7(b) we can see that for 2000 Hz the u_r displacement has already significantly increased all over the cross section. It only remains zero in the center of the cylinder. At the same time the u_z displacement decreases but keeps its maximum value in the center.

For a higher frequency [5000 Hz; Fig. 7(c)] it can be observed that the shape of the displacement profiles evolves slowly toward the typical pattern of Rayleigh modes. Close to the surface ($r = 0.85-1$ m) the motion is already Rayleigh-like. Only toward the center of the bar is the u_z component still relatively strong.

Finally in Fig. 7(d) we get the typical particle motion profile of Rayleigh waves. In contrast to Fig. 7(c) obviously the amplitudes of both displacement components decrease significantly for $r < 0.8$ m.

VI. CONCLUSIONS

We extended and implemented the spectral method for propagation of axisymmetric modes in a cylindrical bar. The method was also generalized to n-layered cylindrical fluid–solid structures. Numerical examples for a free solid cylinder and a fluid-filled tube were given in the form of dispersion curves and particle displacement profiles. Traditional techniques require finding complex roots of nonlinear equations that involve special functions. In contrast, spectral method demands only solving generalized eigenvalue problem without involving special functions. This represents a great simplification that becomes particularly advantageous for complex rheologies like viscoelastic, anisotropic, and poroelastic structures.

There are a lot of directions for further work. One scope is the extension to more complicated media like viscoleasticity and poroelasticity. The approach can also be extended for anisotropic and heterogeneous media. Of great importance will also be to allow unbounded structures, representing a borehole surrounded by infinite rock formation. Finally it would be of great importance to be able to compute the full wave form using the spectral method.

ACKNOWLEDGMENTS

The authors are grateful to Professor Boris Kasthan (St. Petersburg State University, Russia), who suggested the idea of applying the spectral method to the problem at hand. The authors also thank Shell International Exploration and Production for support of this work and Alexander Sidorov (St. Petersburg State University, Russia) for the computation of some dispersion curves using his *root-finding* program. Professor Richard Craster (Imperial College London) is thanked for his helpful advice.

[1] L. Pochhammer, "On the propagation velocities of small oscillations in an unlimited isotropic circular cylinder," J. Reine Angew. Math. **81**, 324–336 (1876).
[2] C. Chree, "The equations of an isotropic elastic solid in polar and cylindrical coordinates, their solutions and applications," Trans. Cambridge Philos. Soc. **14**, 250–369 (1889).
[3] A. E. H. Love, *A Treatise on the Mathematical Theory of Elasticity* (Dover, New York, 1944).
[4] H. Kolsky, *Stress Waves in Solids* (Dover, New York, 1963).
[5] D. Bancroft, "The velocity of longitudinal waves in cylindrical bars," Phys. Rev. **59**, 588–593 (1941).
[6] D. C. Gazis, "Three-dimensional investigation of the propagation of waves in hollow circular cylinders. I. Analytical foundation," J. Acoust. Soc. Am. **31**, 568–573 (1959).
[7] D. C. Gazis, "Three-dimensional investigation of the propagation of waves in hollow circular cylinders. II. Numerical results," J. Acoust. Soc. Am. **31**, 573–578 (1959).
[8] J. A. McFadden, "Radial vibrations of thick-walled hollow cylinders," J. Acoust. Soc. Am. **26**, 714–715 (1954).
[9] V. A. Del Grosso and R. E. McGill, "Remarks on 'Axially symmetric vibrations of a thin cylindrical elastic shell filled with nonviscous fluid' by Ram Kumar, Acustica 17 [1968], 218," Acustica **20**, 313–314 (1968).
[10] T. Lin and G. Morgan, "Wave propagation through a fluid contained in a cylindrical, elastic shell," J. Acoust. Soc. Am. **28**, 1165–1176 (1956).
[11] S. I. Rubinow and J. B. Keller, "Wave propagation in a fluid-filled tube," J. Acoust. Soc. Am. **50**, 198–223 (1971).
[12] V. N. R. Rao and J. K. Vandiver, "Acoustics of fluid filled boreholes with pipe: Guided propagation and radiation," J. Acoust. Soc. Am. **105**, 3057–3066 (1997).
[13] G. W. Morgan and J. P. Kiely, "Wave propagation in a viscous liquid contained in a flexible tube," J. Acoust. Soc. Am. **26**, 323–328 (1954).
[14] J. Vollmann, R. Breu, and J. Dual, "High-resolution analysis of the complex wave spectrum in a cylindrical shell containing a viscoelastic medium. II. Experimental results versus theory," J. Acoust. Soc. Am. **102**, 909–920 (1997).
[15] J. Vollmann and J. Dual, "High-resolution analysis of the complex wave spectrum in a cylindrical shell containing a viscoelastic medium. I. Theory and numerical results," J. Acoust. Soc. Am. **102**, 896–908 (1997).
[16] J. G. Berryman, "Dispersion of extensional waves in fluid-saturated porous cylinders at ultrasonic frequencies," J. Acoust. Soc. Am. **74**, 1805–1812 (1983).
[17] G. H. F. Gardner, "Extensional waves in fluid-saturated porous cylinders," J. Acoust. Soc. Am. **34**, 36–39 (1962).
[18] C. J. Wisse, D. M. J. Smeulders, G. Chao, and M. E. H. van Dongen, "Guided wave modes in porous cylinders: Theory," J. Acoust. Soc. Am. **122**, 2049–2056 (2007).
[19] A. T. I. Adamou and R. V. Craster, "Spectral methods for modelling guided waves in elastic media," J. Acoust. Soc. Am. **116**, 1524–1535 (2004).
[20] J. D. Achenbach, *Wave Propagation in Elastic Solids* (North Holland, Amsterdam, 1973).
[21] J. A. C. Weideman and S. C. Reddy, "A MATLAB differentiation matrix suite," ACM Trans. Math. Softw. **26**, 465–519 (2000).
[22] R. M. Davies, "A critical study of Hopkinson pressure bar," Proc. R. Soc. London, Ser. A **240**, 375–457 (1948).